Opposing activities of two novel members of the IL-1 ligand family regulate skin inflammation

Hal Blumberg,[1] Huyen Dinh,[1] Esther S. Trueblood,[2] James Pretorius,[4] David Kugler,[1] Ning Weng,[3] Suzanne T. Kanaly,[2] Jennifer E. Towne,[1] Cynthia R. Willis,[1] Melanie K. Kuechle,[5] John E. Sims,[1] and Jacques J. Peschon[1]

[1]Department of Inflammation, [2]Department of Pathology, [3]Department of Biostatistics, Amgen, Seattle, WA 98119
[4]Department of Pathology, Amgen, Thousand Oaks, CA 91320
[5]Department of Dermatology, University of Washington School of Medicine, Seattle, WA 98105

The interleukin (IL)-1 family members IL-1α, -1β, and -18 are potent inflammatory cytokines whose activities are dependent on heterodimeric receptors of the IL-1R superfamily, and which are regulated by soluble antagonists. Recently, several new IL-1 family members have been identified. To determine the role of one of these family members in the skin, transgenic mice expressing *IL1F6* in basal keratinocytes were generated. *IL1F6* transgenic mice exhibit skin abnormalities that are dependent on IL-1Rrp2 and IL-1RAcP, which are two members of the IL-1R family. The skin phenotype is characterized by acanthosis, hyperkeratosis, the presence of a mixed inflammatory cell infiltrate, and increased cytokine and chemokine expression. Strikingly, the combination of the IL-1F6 transgene with an *IL1F5* deficiency results in exacerbation of the skin phenotype, demonstrating that IL-1F5 has antagonistic activity in vivo. Skin from *IL1F6* transgenic, *IL1F5*$^{-/-}$ pups contains intracorneal and intraepithelial pustules, nucleated corneocytes, and dilated superficial dermal blood vessels. Additionally, expression of *IL1RL2*, *-1F5*, and *-1F6* is increased in human psoriatic skin. In summary, dysregulated expression of novel agonistic and antagonistic IL-1 family member ligands can promote cutaneous inflammation, revealing potential novel targets for the treatment of inflammatory skin disorders.

CORRESPONDENCE
Hal Blumberg:
blumberh@amgen.com

Abbreviations used: AcP, accessory protein; bp, binding protein; HE, hematoxylin and eosin; IHC, immunohistochemistry; ICAM, intercellular adhesion molecule; ISH, in situ hybridization; MAP, multiple analyte panel; P, postnatal day.

IL-1α (IL-1F1) and IL-1β (IL-1F2) are related cytokines involved in inflammation in a variety of tissues and diseases (1, 2). Both are ligands for a heterodimeric receptor composed of the type 1 IL-1R (IL-1R) and IL-1R accessory protein (AcP; IL-1RAcP) (3). Either IL-1α or β can bind to IL-1R, but this alone does not activate signal transduction. Binding of the ligands to IL-1R results in recruitment of AcP to the complex, resulting in juxtaposition of intracellular IL-1R and AcP TIR (Toll/IL-1R) domains, and activation of signal transduction (2). Another related ligand, IL-1R antagonist (IL-1ra and IL-1F3), competes with IL-1α and -1β for binding to IL-1R. The IL-1R–IL-1ra complex cannot recruit AcP, and is incapable of signaling (4). Type II IL-1R and a soluble form of AcP are involved in additional layers of IL-1 regulation (5, 6).

IL-18 (IL-1F4) is another IL-1 ligand family member involved in inflammation (7, 8). IL-18R and -18RAcPL comprise the functional IL-18R (9). A natural antagonist of this system, IL-18–binding protein (IL-18bp), is not an IL-1 family member and acts by sequestering IL-18, preventing it from binding to its receptor (10). Therefore, IL-18bp and -1ra act to antagonize their respective cytokines by distinct mechanisms.

Several IL-1 ligand and receptor family members have been implicated in cutaneous inflammation. Transgenic mice expressing *IL1A* from the keratin 14 (K14) promoter develop focal inflammatory skin lesions, hair loss, and scaling. At the histological level, the transgenic mice have hyperkeratosis and dermal inflammation mainly

S.T. Kanaly's present address is Dept. of Pathology, Allergan, Inc., Irvine, CA 92612.

J.J. Peschon's present address is Institute for Systems Biology, Seattle, WA 98103.

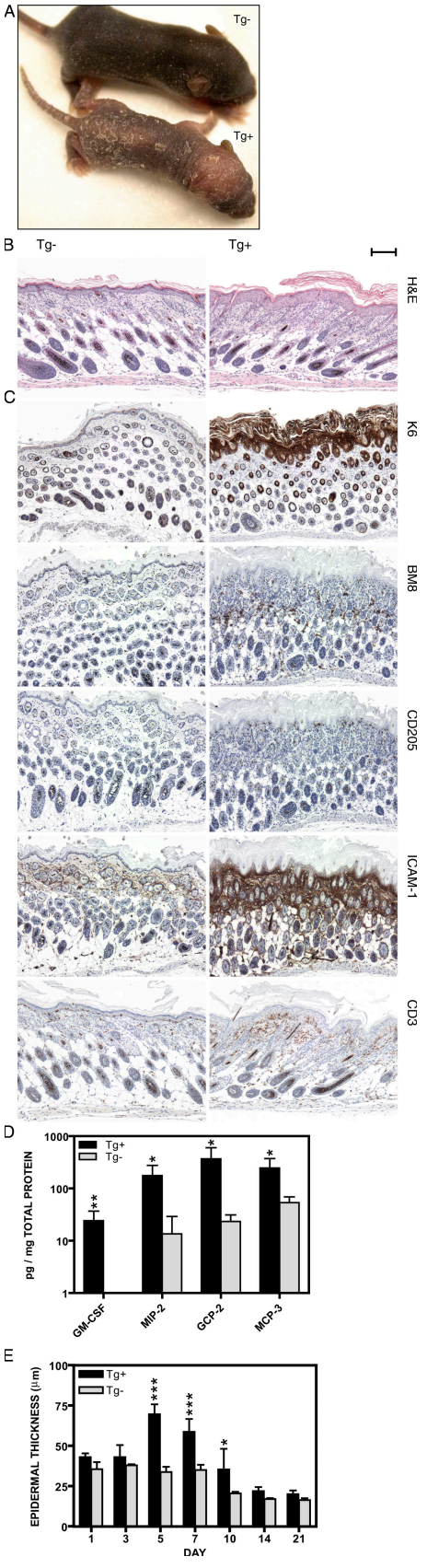

composed of macrophages, but no alteration in epidermal thickness (11). Transgenic mice expressing *IL18* from the keratin 5 promoter exhibit many features of atopic dermatitis, including acanthosis; an infiltrate composed of eosinophils, neutrophils, and mast cells; an increase in serum IgE levels; and an increase in B cells in the draining lymph node (12). In a BALB/c genetic background, *IL1RN*-deficient mice have histological features in common with psoriasis (13). Mice deficient in *IL1R1*, *IL1RAP*, *IL18R1*, and *IL18RAP* have no overt skin abnormalities (14–18).

Genes encoding several IL-1–related ligands (from *IL1F5* to *IL1F10*) have been discovered and map to human chromosome 2q, the same locus as *IL1A*, *-1B*, and *-1RN* (1, 19–25). These IL-1F ligands lack signal sequences, and only IL-1F7 contains a proregion. Phylogenetic analysis indicates that *IL1F5* and *-1F10* are most closely related to *IL1RN* (24, 25). *IL1F6*, *-1F*8, and *-1F9* comprise a separate triplet branch of the phylogenetic tree.

There are now 10 known members of the IL-1R family (2). IL-1Rrp2 (RP2) was originally identified as an IL-1R family member expressed in the brain (26). IL-1F9 was demonstrated to activate signal transduction in an RP2-dependent manner (27). In addition, IL-1F9 activation of RP2 was antagonized by IL-1F5. These results have been extended by the demonstration that IL-1F6 and -1F8, in addition to IL-1F9, activate signal transduction pathways and require both RP2 and AcP (28). Quantitative RT-PCR analysis indicates that *IL1F6*, *-1F8*, and *-1F9* are expressed in a restricted manner, primarily in the skin and in other epithelial tissues, whereas *IL1RL2* and *IL1RAP* are more widely expressed (unpublished data) (28).

We report that transgenic expression of *IL1F6* in basal keratinocyte cells results in cutaneous alterations in both the

Figure 1. K14/*IL1F6* transgenic pups have skin abnormalities. (A) K14/*IL1F6* transgenic pups have flaky skin, ringtail, and are runted. The gross phenotype of a K14/*IL1F6* transgenic (Tg^+) pup and a nontransgenic (Tg^-) cagemate at 7 d of age is shown. (B) Skin from K14/*IL1F6* transgenic pups is hyperkeratotic, acanthotic (increased epidermal thickness), and contains a dermal inflammatory cell infiltrate. HE staining of skin from a K14/*IL1F6* Tg^+ and Tg^- pup at 7 d of age is shown. (C) Skin from K14/*IL1F6* transgenic pups has increased expression of keratin 6 and ICAM-1, and an increased number of $BM8^+$ macrophage, $CD205^+$ Langerhans or dermal dendritic cells, and $CD3^+$ T lymphocytes relative to skin from nontransgenic littermate control pups. $CD205^+$ staining most likely represents Langerhans cells, as the majority of the signal is epidermal. IHC staining of skin from K14/*IL1F6* Tg^+ and Tg^- pups at 7 d of age with specific antibodies is shown. Bar, 100 μm. (D) Chemokines and cytokine protein levels are elevated in the skin of K14/*IL1F6* transgenic pups compared with nontransgenic littermate pups. Skin was isolated from 7-d-old K14/*IL1F6* Tg^+ and Tg^- pups, protein extracts were prepared, normalized to total protein, and analyzed by Rules Based Medicine MAP profiling. MIP2, CXCL8 (IL-8); GCP2, CXCL6; MCP-3, CCL7. (E) Epidermal thickness is increased in the skin of K14/*IL1F6* transgenic pups at P5, 7, and 10 compared with nontransgenic cagemate control pups. Skin was isolated from K14/*IL1F6* Tg^+ and Tg^- pups, stained with HE, and epidermal thickness was determined by histomorphometric analysis. Error bars in C and D represent the mean ± the SD. *, $P < 0.05$; **, $P < 0.01$; ***, $P < 0.001$.

epidermis and dermis. Importantly, we demonstrate that the severity of the skin abnormalities is increased in *IL1F5*–deficient mice, providing genetic evidence that IL-1F5 possesses antagonistic activity in vivo. We also demonstrate that *IL1RL2*, *IL1F5*, and *IL1F6* expression is increased in human psoriatic skin, thus suggesting a possible connection between the mouse skin phenotype and human pathophysiology.

RESULTS

Expression of *IL1F6* in skin results in cutaneous inflammation

The human K14 promoter was used to express mouse *IL1F6* in basal keratinocytes in transgenic mice. Nine founders were obtained, one of which had severe skin abnormalities and was killed. This mouse had the highest *IL1F6* expression in skin of the founders. The next four highest expressers were developed into lines, all of which had a similar gross phenotype. The studies reported in this work were performed on a line with at least 70-fold higher mRNA levels in skin relative to the endogenous *IL1F6* mRNA level (unpublished data). K14/*IL1F6* pups were small, had flaky skin, and developed ringtail (Fig. 1 A). The skin phenotype was first observable at postnatal day (P) 5, was most severe at P7, and was overtly resolved by P21. However, recurrence of skin lesions, predominantly on the face, snout, and ears, developed in K14/*IL1F6* mice at 6 mo of age.

Histological analysis on transgenic pups at P7 demonstrated acanthosis, hyperkeratosis, and a mixed inflammatory cell infiltrate in the dermis composed mainly of neutrophils, macrophages, and lymphocytes (Fig. 1 B). Histological changes in keratinocytes and immune cells were analyzed by immunohistochemistry (IHC). Increased immunoreactivity was observed in markers for keratinocyte hyperproliferation (keratin 6), macrophages (BM8), epidermal Langerhans and dermal dendritic cells (CD205), inflammation (intercellular adhesion molecule 1 [ICAM-1]), and T lymphocytes (CD3; Fig. 1 C). Levels of a variety of cytokines and chemokines in skin protein extracts were compared in 1-wk-old K14/*IL1F6* pups and their nontransgenic littermates. Elevated levels of GM-CSF, MIP-2, GCP-2, and MCP-3 were observed in the transgenic skin relative to the nontransgenic control skin (Fig. 1 D).

To determine how the skin phenotype develops, we compared skin from K14/*IL1F6* pups to their nontransgenic littermates at 1, 3, 5, 7, 10, 14, and 21 d after birth by histopathological analysis. During this time period, the mouse epidermis normally decreases in epidermal thickness. The maximal increase in epidermal thickness in K14/*IL1F6* skin relative to nontransgenic skin was observed at P5 (Fig. 1 E). In contrast, the presence of a mixed dermal inflammatory infiltrate reached its peak at P7 (unpublished data). Resolution of the histopathological skin abnormalities began between P7 and 10, and progressed to normal skin by P21.

Resolution of the K14/*IL1F6* skin phenotype

We considered several possible hypotheses to explain the resolution of the K14/*IL1F6* skin phenotype that occurs between P7 and 21; silencing of the *IL1F6* transgenic expression, decreased expression of the required RP2 and/or AcP receptor subunits (see Fig. 3), and increased expression of the IL-1F5 antagonist (see Fig. 4). Quantitative RT-PCR analysis was performed on *IL1F6*, *IL1RL2*, *IL1RAP*, and *IL1F5* in the skin from transgenic and nontransgenic pups at P1, 3, 5, 7, 10, 14, and 21. *IL1F6* mRNA is expressed at higher levels in transgenic pup skin than in the nontransgenic pup skin at all time points (Fig. 2 A). However, transgenic *IL1F6* expression decreases over the 21-d time course. Expression levels of *IL1F5*, *-1F8*, and *-1F9* are increased in the K14/*IL1F6* transgenic skin relative to the nontransgenic skin, and decreased from P1 to P21 in parallel with *IL1F6* transgene expression (Fig. 2 A). *IL1RL2* mRNA levels are slightly higher in transgenic skin than in nontransgenic skin at P1 and 3, but not at later time points (Fig. 2 B). *IL1RAP* mRNA levels are not altered at any time point by the presence of the transgene (Fig. 2 B). Expression of *IL23A*, *CSF2*, *TNF*, *IL1A*, *CCL2*, *KRT14*, *CXCL2*, *HBEGF*, and *AREG* mRNA was increased at specific time points in the transgenic skin, relative to the nontransgenic control skin (Fig. 2 C). However, their expression decreases as K14/*IL1F6* transgene expression diminishes (Fig. 2 C). Therefore, decreased expression of the *IL1F6* transgene, *IL1F8*, *IL1F9*, *IL1RL2*, and inflammatory cytokines and chemokines is observed over the first 3 wk of age.

To further characterize the decreased expression of the K14/*IL1F6* transgene over time, IHC was performed on IL-1F6 and K14. The following three time points were selected for analyses: P1 (initiation of transgene-dependent expression changes), P5 (peak of increased epidermal thickness induced by transgene expression), and P10 (after resolution of the skin phenotype has begun). Expression of IL-1F6 was observed throughout the epidermis at P1 and P5 in the transgenic skin, with the highest levels observed in the superficial epidermis (Fig. 2 D). Expression of IL-1F6 in nontransgenic pup skin was only in the superficial layer at P1 and P5. In contrast, IL-1F6 expression in transgenic skin at P10 was only observed in the superficial epidermis, and it was similar in intensity to the endogenous, nontransgenic IL-1F6 level. To investigate expression of a skin marker at these same time points, we chose K14, as its promoter was used to drive IL-1F6 expression in the transgenic mice. K14 protein is found throughout the epidermis at P1 and 5 in transgenic skin, although a predominance of basal layer expression was observed at P5 (Fig. 2 E). However, K14 protein was only observed in the basal layer in the transgenic skin at P10, which is its normal localization as shown in the nontransgenic skin (Fig. 2 E). Therefore, it appears that *IL1F6* transgene expression is silenced in parallel with the phenotypic resolution.

Receptor requirement for K14/*IL1F6* skin phenotype

RP2 and AcP were shown to be required for activation of signal transduction in vitro by IL-1F6 (28). To determine whether these receptor subunits were required for the skin alterations in K14/*IL1F6* pups, transgenic mice were crossed

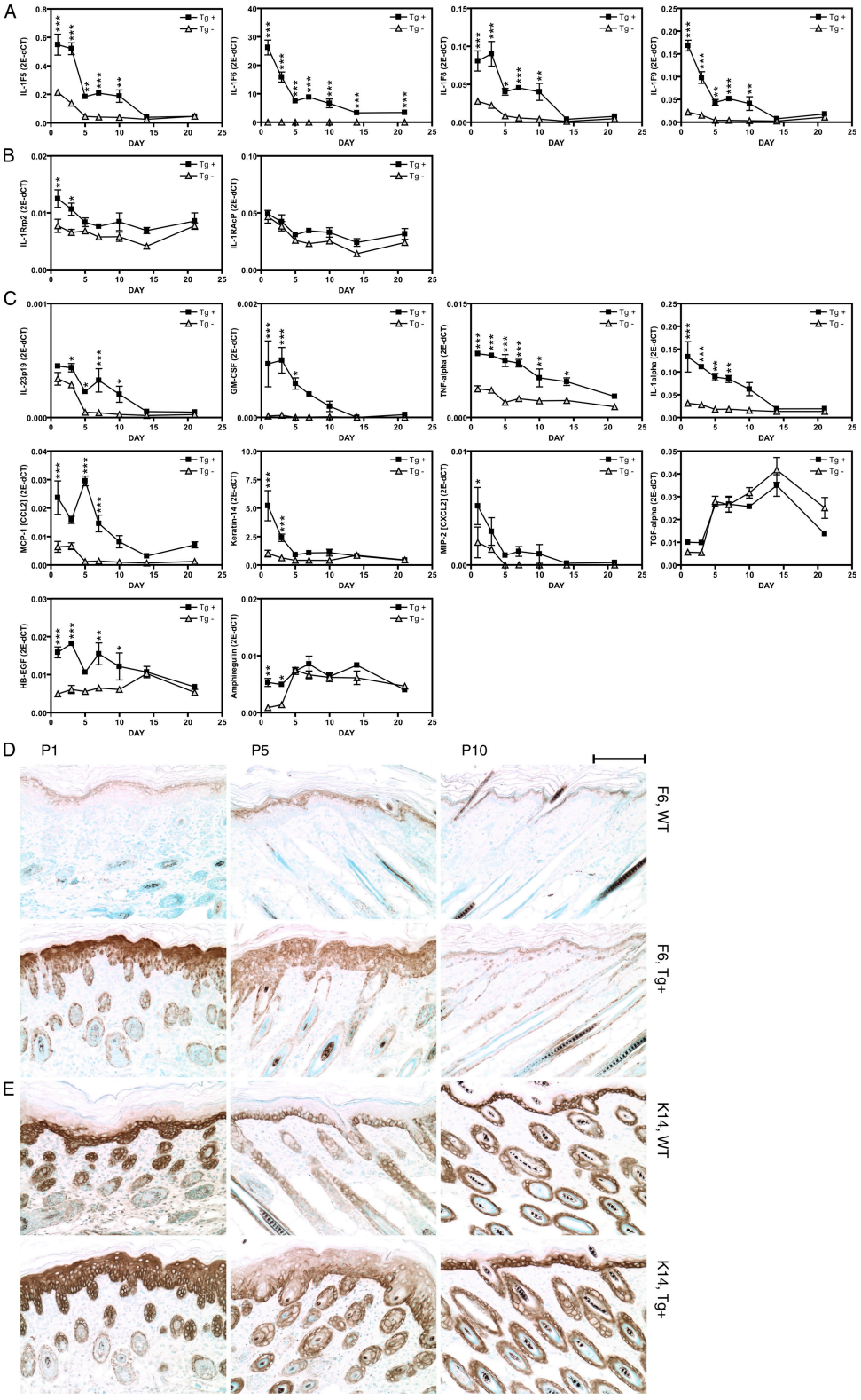

Figure 2. Quantitative RT-PCR and IHC analyses demonstrate reduced expression of IL-1F6 as the skin phenotype resolves. (A) Expression of *IL1F5*, *-1F6*, *-1F8*, and *-1F9* in the skin decreases over the P1–21 time course. (B) Expression of *IL1RL2* is elevated in transgenic skin relative to control skin at P1 and 3. Expression of *IL1RL2* at P5–21, and expression of *IL1RAP* from P1–21 is not different in transgenic and nontransgenic skin. (C) Expression of *IL23A*, *CSF2*, *TNF*, *IL1A*, *CCL2*, *KRT14*, *CXCL2*, *TGA2*, *HBEGF*, and *AREG* is given in both transgenic and nontransgenic skin from P1 to 21. Total skin RNA was isolated from K14/*IL1F6* transgenic and nontransgenic pups ($n = 3$) and was analyzed by quantitative RT-PCR. Expression of specific genes is relative to

into *IL1RL2*- or *IL1RAP*-deficient backgrounds. Mice deficient in *IL1RL2* were generated as described in the Materials and methods. Mice lacking *IL1RL2* were born at the predicted Mendelian ratios from heterozygous intercrosses and displayed no overt phenotypes on C57BL/6; 129 hybrid, C57BL/6, or FVB genetic backgrounds. Mice deficient in *IL1RL2* or *IL1RAP* have normal skin in an unchallenged context. Transgenic pups carrying the K14/*IL1F6* transgene and lacking the receptor subunit ($^{-/-}$) were compared with littermates that were transgenic and were heterozygous ($^{+/-}$) or wild-type ($^{+/+}$) for the receptor subunit. Expected Mendelian ratios were observed for all crosses. Pups were scored by their gross phenotype and by histopathological analyses at P7. Nontransgenic pups had normal skin, whereas transgenic pups that were *IL1RL2*$^{+/+}$, *IL1RAP*$^{+/+}$, *IL1RL2*$^{+/-}$, or *IL1RAP*$^{+/-}$ had a skin phenotype. However, transgenic pups lacking *IL1RL2* or *IL1RAP* did not exhibit a phenotype (Fig. 3, A and B). Therefore, *IL1RL2* and *IL1RAP* are required for the K14/*IL1F6* skin phenotype.

To provide further support for the essential role of RP2 in mediating IL-1F6 activity, intraperitoneal injections of a neutralizing monoclonal antibody against mouse RP2 (M616) and an isotype-matched control antibody in K14/*IL1F6* newborn pups were performed. Half of each litter was injected with 50 μg M616 on P1, 3, and 5, whereas the rest of the litter was marked and injected with 50 μg control antibody. Pups were killed on P7, and were subjected to genotyping and histological analyses. The skin phenotype was blocked by M616 administration, but not by treatment with a control antibody, confirming the RP2 requirement (Fig. 3 C).

The K14/*IL1F6* transgene was crossed into an *IL1R1*-deficient background to determine if this receptor is required for the skin phenotype. *IL1R1*-deficient mice have no skin abnormalities in an unchallenged context. Expected Mendelian ratios were observed. K14/*IL1F6* transgenic pups lacking *IL1R1* exhibit a skin phenotype similar in severity to K14/*IL1F6* pups containing *IL1R1* (Fig. 3 D). Therefore, *IL1R1* is not required for the K14/*IL1F6* skin phenotype.

Immune requirements for the K14/*IL1F6* skin phenotype

TNF-α is an important cytokine in skin inflammation, and its blockade is an effective treatment for psoriasis (29). TNF-α mRNA is elevated in the skin of K14/*IL1F6* pups from P1-P14 (Fig. 2 C). To determine if the K14/*IL1F6* transgenic skin phenotype is dependent on TNF-α, K14/*IL1F6* pups were treated with TN3-19.12 (30), a neutralizing antibody against mouse TNF-α. Transgenic pups treated with anti–TNF-α have a statistically significant decrease in epidermal thickness (Fig. 4 A) and a much more dramatic reduction in the amount of dermal immune infiltrate (Fig. 4 B) compared with pups treated with a control antibody. Additionally, K14/*IL1F6*, *TNFRSF1A*$^{-/-}$ (p55) pups had a similar decrease in epidermal thickness and dermal infiltrate compared with K14/*IL1F6*, *TNFRSF1A*$^{+/+}$ (p55) pups (unpublished data). Therefore, TNF-α and *TNFRSF1A* are not required for the K14/*IL1F6* skin phenotype, but they do modulate the severity of the skin lesion, especially the amount of dermal inflammation.

Expression of chemokines involved in neutrophil mobilization is elevated in the skin of K14/*IL1F6* pups (Fig. 1 D and Fig. 2 C), leading to the recruitment of neutrophils to the dermis (Fig. 1 B). To understand the functional role of neutrophils in the transgenic skin, pups were treated with the neutrophil-depleting antibody anti-Gr1 (31) or with an isotype-matched control antibody. Most of the neutrophils in the skin were depleted with anti-Gr1 treatment relative to those treated with the control antibody (Fig.4 D). However, some neutrophils were still detected in the skin. Decreased neutrophils numbers with anti-Gr1 treatment resulted in a lower inflammation severity ranking (Fig. 4 C), but there was little effect on the epidermal thickness (unpublished data). Because of incomplete depletion, we cannot prove that neutrophils are dispensable for the generation of the IL-1F6–induced skin abnormalities. However, we can conclude that elimination of the majority of skin neutrophils primarily has its effect on the dermal infiltrate.

There is an increase in CD3$^+$ T lymphocytes in the skin of K14/IL-1F6 pups compared with the skin of nontransgenic littermates (Fig. 1 C). To determine the role that lymphocytes play in the generation of the skin phenotype, the K14/*IL1F6* transgene was crossed onto a *RAG2*-deficient background (32). IHC with anti-CD3 demonstrated that T lymphocytes were indeed absent in the skin of K14/*IL1F6*, *RAG2*$^{-/-}$ pups (Fig. 4 E). No differences were observed in the skin at the gross level, and only a slightly decreased severity between K14/*IL1F6*, *RAG2*$^{-/-}$ pups and K14/*IL1F6*, *RAG2*$^{+/-}$ pups was noted histologically. In addition, the expression of the inflammatory marker ICAM-1 was not altered (Fig. 4 E). Therefore, mature lymphocytes are also not required for the observed skin abnormalities in the K14/*IL1F6* transgenic pups.

Exacerbation of the K14/*IL1F6* skin phenotype in *IL1F5*$^{-/-}$ and *-1F5*$^{+/-}$ mice

IL-1F5 antagonizes the RP2-dependent signal transduction in vitro in response to IL-1F9 (27). Because IL-1F6 has similar activity to IL-1F9 in vitro (28), we tested whether IL-1F5 can also block the effect of this ligand. IL-1F5 antagonized IL-1F6 activity in a variety of in vitro assays (unpublished data). Substantial inhibition was observed at an equimolar IL-1F5/-1F6 ratio, which is consistent with published results (27).

β-actin. *, $P < 0.05$; **, $P < 0.01$; ***, $P < 0.001$. Error bars in A–C represent the mean ± the SD. (D) Protein expression of IL-1F6 in K14/*IL1F6* transgenic pup skin is elevated at P1 and P5 relative to nontransgenic control skin, but is decreased to the endogenous level by P10. (E) K14 protein was detected throughout the epidermis in transgenic pups at P1 and 5, and is observed only in the basal layer at P10. Skin samples were fixed in neutral buffered formalin, sectioned, analyzed by IHC using a monoclonal antibody against mouse IL-1F6 or a polyclonal antibody against K14. Bar, 100 μm.

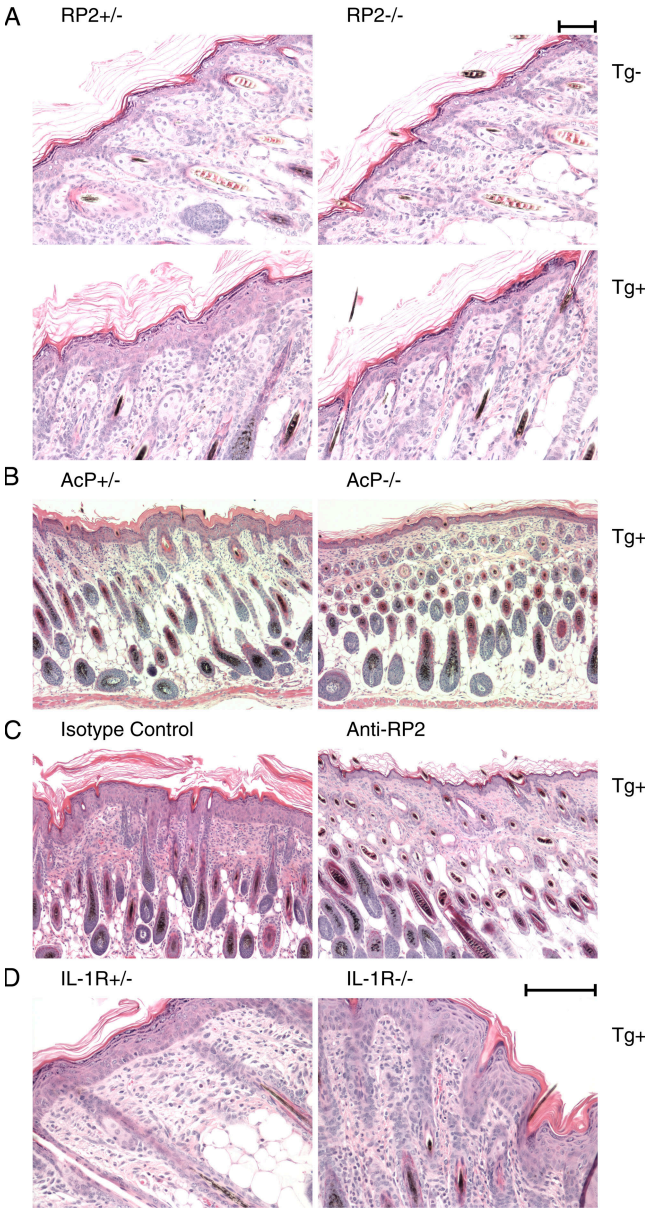

Figure 3. RP2 and AcP are required receptor subunits for the K14/*IL1F6* skin phenotype. (A) Skin from 7-d-old K14/*IL1F6*, *IL1RL2*$^{+/-}$ pups exhibits hyperkeratosis, increased epidermal thickness, and the presence of a dermal infiltrate compared with skin from nontransgenic littermates. In contrast, skin from 7-d-old K14/*IL1F6*, *IL1RL2*$^{-/-}$ pups does not exhibit any of the skin abnormalities. (B) Skin from 7-d-old K14/*IL1F6*, AcP$^{-/-}$ pups lack the skin phenotype of K14/*IL1F6*, AcP$^{+/-}$ littermates. (C) K14/*IL1F6* transgenic pups injected intraperitoneally with a blocking antibody against mouse RP2 (M616) lack the skin phenotype observed in K14/*IL1F6* littermates treated with an isotype-matched control antibody. HE staining shown is from skin of 7-d-old pups. (D) Skin from 7-d-old K14/*IL1F6*, IL-1R$^{-/-}$ pups has equivalent or more severe skin abnormalities than skin from K14/*IL1F6*, IL-1R$^{+/-}$ littermates. Images from nontransgenic pup skin in B and D are not shown, but are similar to those in A. Bars, 100 μm.

To study whether IL-1F5 can affect the severity of the K14/*IL1F6* skin phenotype, mice deficient in *IL1F5* were generated (see Materials and methods) and analyzed either alone or in combination with the K14/*IL1F6* transgene. A similar analysis of the *IL1F5*-deficient mice was performed as described for the *IL1RL2*-deficient mice, and no overt phenotypes, histopathological abnormalities, or immune cell changes were observed. A genetic cross was performed between K14/*IL1F6*, *IL1F5*$^{+/-}$ mice and *IL1F5*$^{-/-}$ mice. Genotyping of the resulting pups at 3 wk of age indicated that the K14/*IL1F6*, *IL1F5*$^{-/-}$ combination was dramatically underrepresented, with only 1 pup of this genotype out of 109 total pups surviving at weaning. The other three resulting genotypes (K14/*IL1F6*, *IL1F5*$^{+/-}$; *IL1F5*$^{-/-}$; and *IL1F5*$^{+/-}$) were found in roughly equal numbers. We recovered 13 dead pups from these crosses between P5 and 10, and all 13 were K14/*IL1F6*, *IL1F5*$^{-/-}$. These pups had milk in their stomachs, yet were runted and had a dehydrated appearance. Normal skin barrier function as assessed by a dye exclusion assay (33) was observed in K14/*IL1F6*, *IL1F5*$^{-/-}$ at both embryonic day 18.5 and P3 (unpublished data). The surviving K14/*IL1F6*, *IL1F5*$^{-/-}$ mouse that reached adulthood subsequently developed severe skin abnormalities. The visible skin phenotype of K14/*IL1F6*, *IL1F5*$^{-/-}$ and K14/*IL1F6*, *IL1F5*$^{+/-}$ pups was apparent by P3, whereas K14/*IL1F6*, *IL1F5*$^{+/+}$ pups do not have gross skin changes until P5 (Fig. 5 A and not depicted). K14/*IL1F6*, *IL1F5*$^{-/-}$ pups are much smaller than their littermates and have severe skin abnormalities resembling blisters. K14/*IL1F6*, *IL1F5*$^{+/-}$ pups also have extensive regions of thick, scaly skin. Histological analysis reveals intracorneal and intraepithelial pustules, parakeratotic and orthokeratotic hyperkeratosis, dilated superficial dermal blood vessels, and a mixed dermal inflammatory infiltrate (Fig. 5 B). Therefore, the combination of the K14/*IL1F6* transgene and *IL1F5* deficiency results in increased severity of the skin phenotype and neonatal lethality.

Intraperitoneal injection of newborn K14/*IL1F6*, *IL1F5*$^{-/-}$ pups with 50 μg M616 at P1, 3, and 5 rescued the neonatal lethality. However, upon cessation of antibody treatment, adult K14/*IL1F6*, *IL1F5*$^{-/-}$ and K14/*IL1F6*, *IL1F5*$^{+/-}$ mice develop severe lesions on their face, neck, and ears by 4–6 wk of age. Histological analysis of the K14/*IL1F6*, *IL1F5*$^{-/-}$ and K14/*IL1F6*, *IL1F5*$^{+/-}$ adult skin demonstrates similar features as seen in the pups, with the presence of focal "plaques" interspersed with regions of normal skin (Fig. 5 C and not depicted). High magnification images in Fig. 5 D show parakeratotic hyperkeratosis and dilated superficial dermal blood vessels with a mixed inflammatory infiltrate.

IL1RL2, *IL1F6*, and *IL1F5* expression is increased in human psoriatic skin

Psoriatic plaques and nonlesional skin from 10 patients were assayed by in situ hybridization (ISH) with probes specific for human *IL1RL2*, *IL1F6*, and *IL1F5*. Elevated, but low-level expression of *IL1RL2* was detected throughout the epidermis in plaques in 9/10 patients, but not in nonlesional

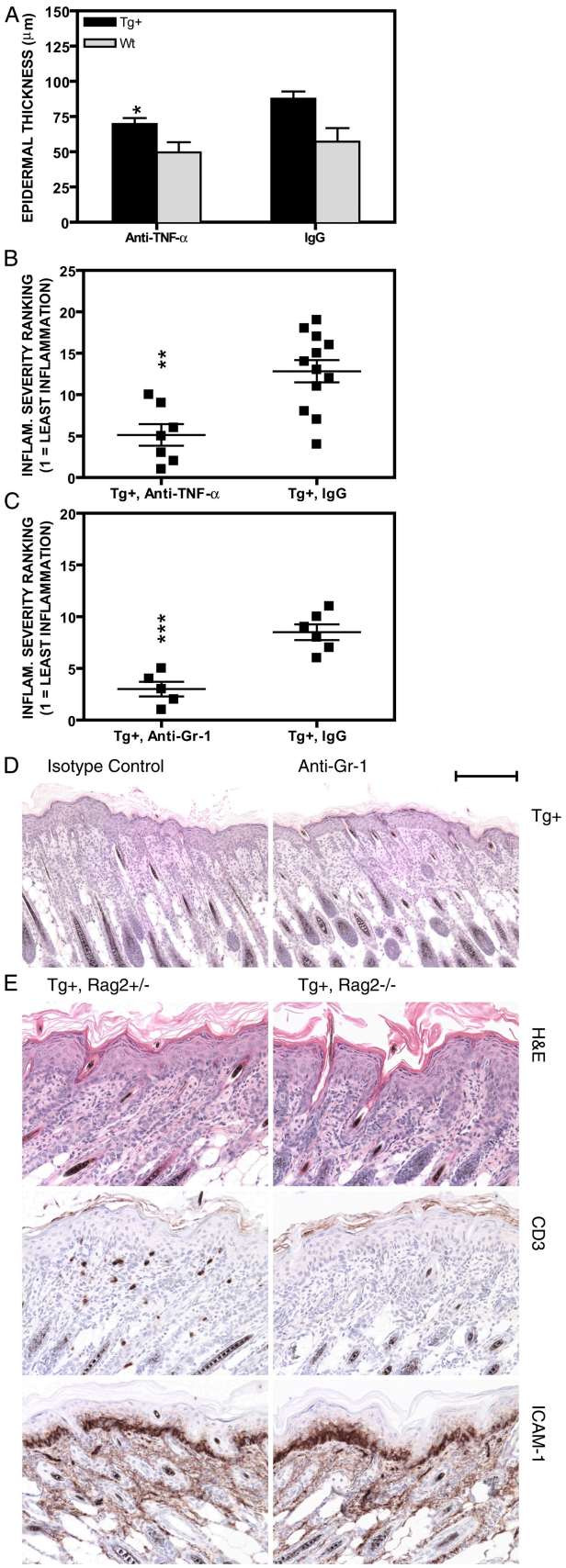

skin (Table I). No *IL1RL2* expression was detected in either plaques or normal skin in the 10th patient. *IL1F6* expression was strongly detected in the superficial layers of the epidermis in plaques from skin in all 10 patients, but was either not detectable or was only weakly detectable in nonlesional skin samples (Fig. 6, A and B; Table I). *IL1F5* is expressed in both psoriatic plaques and in nonlesional skin from all patients (Fig. 6 C, Table I). *IL1F5* expression was found throughout the epidermis, with a stronger signal in the superficial layers. *IL1F5* expression appeared to be higher in plaques compared with nonlesional skin in 3/10 patients, was slightly higher in 4/10 patients, and was unchanged in 3/10 patients. *IL1F5*, *IL1F6*, and *IL1RL2* expression was increased in additional psoriatic skin samples, including samples of pustular psoriasis, and in several samples of the psoriasis-like skin disease pityriasis rubra pilaris, but not in chronic eczematous dermatitis or in nummular dermatitis (unpublished data).

To provide quantitative evidence for the association of *IL1RL2*, *IL1F5*, and *IL1F6* expression with psoriasis, RT-PCR analysis was performed on seven paired psoriatic and nonlesional skin samples. Higher expression of *IL1RL2*, *IL1F5*, and *IL1F6* mRNAs was observed in all psoriatic skin samples compared with their corresponding paired nonlesional skin (Fig. 6 D). In addition, there was a correlation between the expression levels of the three genes in individual patients (unpublished data). We conclude that *IL1RL2*, *IL1F5*, and *IL1F6* expression is increased in psoriasis.

DISCUSSION

The IL-1 ligand superfamily has recently been expanded by the discovery of seven new members (23, 34). Three of these ligands (IL-1F6, -1F8, and -1F9) activate signaling pathways in vitro in an RP2- and AcP-dependent manner (27, 28). However, the in vivo function of these molecules has remained obscure. We demonstrate that transgenic expression of IL-1F6 in basal keratinocytes leads to skin changes affecting both the epidermis and dermis.

Figure 4. Mechanistic requirements for the K14/*IL1F6* skin phenotype. An antibody against TNF-α results in decreased epidermal thickness (A) and decreased dermal inflammation ranking (B) in skin from 7-d-old K14/*IL1F6* transgenic pups ($n = 7$) compared with K14/*IL1F6* transgenic skin from pups treated with a control antibody ($n = 12$). (C) An antibody against CD18 (anti-Gr1) results in a decreased dermal inflammatory ranking in 7-d-old K14/*IL1F6* transgenic pup skin ($n = 5$) compared with a control antibody ($n = 6$). *, $P < 0.05$; **, $P < 0.01$; ***, $P < 0.001$. Error bars represent the mean ± the SEM. (D) HE staining of K14/*IL1F6* transgenic pup skin indicating a reduced dermal inflammation in anti-Gr1 antibody compared with control antibody, but no change in epidermal thickness. (E) *RAG2* is not required for the skin phenotype in K14/*IL1F6* pups. HE staining of skin from 7-d-old K14/*IL1F6*, $RAG2^{+/-}$ and K14/*IL1F6*, $RAG2^{-/-}$ pups is shown. IHC with anti-CD3 demonstrates the absence of mature T lymphocytes in $RAG2^{-/-}$ pups. IHC with anti-ICAM-1 shows that inflammation is not reduced in K14/*IL1F6*, $RAG2^{-/-}$ pups. Bar, 100 μm.

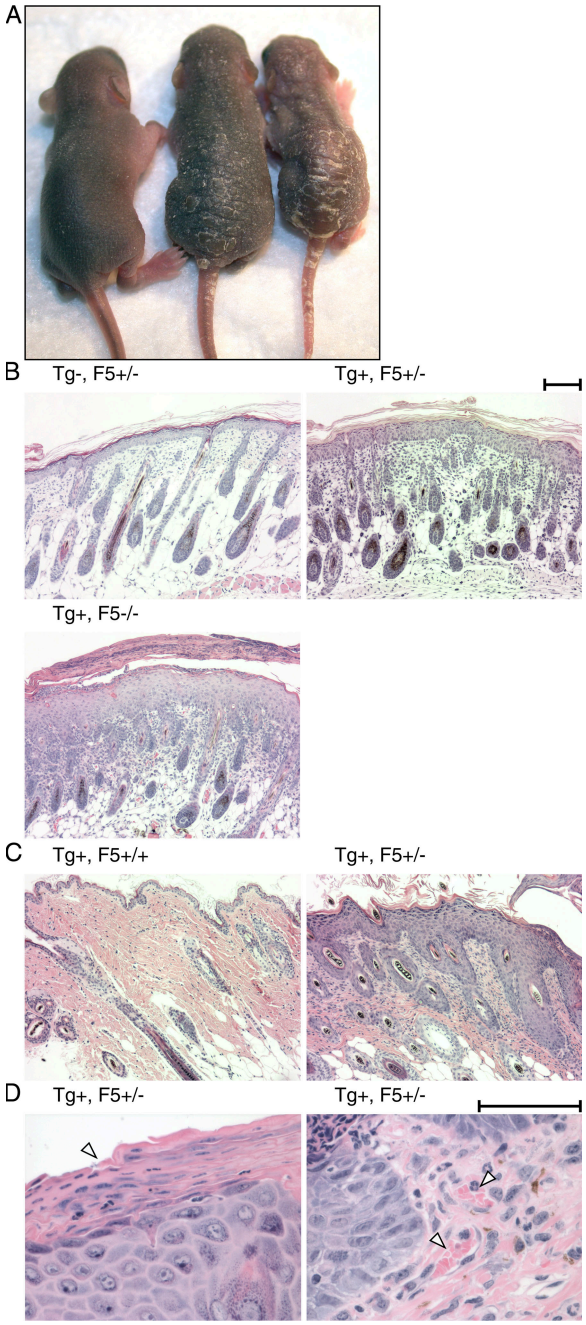

Figure 5. IL-1F5 is an antagonist of IL-1F6 in vivo. (A) K14/*IL1F6* pups with reduced *IL1F5* gene dosage exhibit an altered gross appearance 3 d after birth. The skin phenotype and runting are most severely affected in K14/*IL1F6* Tg^{+}, $IL1F5^{-/-}$ pups. From left to right: K14/*IL1F6* Tg^{-}, $IL1F5^{-/-}$; K14/*IL1F6* Tg^{+}, $IL1F5^{+/-}$; K14/*IL1F6* Tg+, $IL1F5^{-/-}$. (B) K14/*IL1F6* pups with reduced *IL1F5* gene dosage have a thickened epidermis, increased dermal infiltrate, and parakeratosis compared with K14/*IL1F6*, $IL1F5^{+/+}$ pups. HE staining of skin is from 3-d-old pups. (C) Adult K14/*IL1F6*, $IL1F5^{+/-}$ mice have skin abnormalities, whereas K14/*IL1F6*, $IL1F5^{+/+}$ mice do not. HE staining of skin is from 14-wk-old mice. (D, left) K14/*IL1F6*, $IL1F5^{+/-}$ skin exhibits parakeratotic hyperkeratosis; note the nucleated keratinocytes in the corneal layer (arrowhead). (right) K14/*IL1F6*, $IL1F5^{+/-}$ skin contains dilated superficial dermal blood vessels (arrowheads) and a mixed inflammatory infiltrate composed predominantly of neutrophils and macrophages, with fewer lymphocytes and rare eosinophils. Bars, 100 μm.

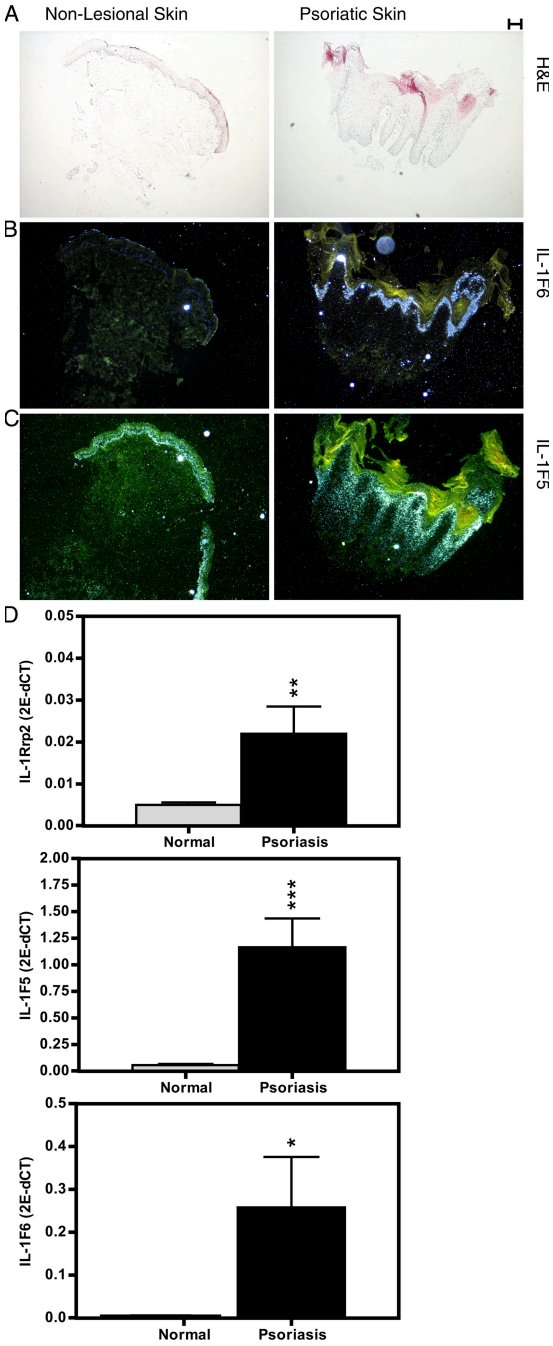

Figure 6. *IL1RL2*, *IL1F5*, and *IL1F6* expression is increased in human psoriatic skin. (A) HE staining of psoriatic skin and nonlesional skin from the same patient are shown. (B) *IL1F6* is up-regulated in psoriatic skin compared with nonlesional skin. *IL1F6* expression is observed only in the upper spinous layer of the epidermis. (C) *IL1F5* expression is detected in both psoriatic skin and nonlesional skin. However, the *IL1F5* ISH signal is stronger in the psoriatic skin than in the nonlesional skin in the example shown. Green staining is autofluorescence from keratins. Bar, 100 μm. (D) Quantitative RT-PCR data for *IL1RL2*, *IL1F5*, and *IL1F6* expression from psoriatic and nonlesional skin from seven patients. *, $P < 0.05$; **, $P < 0.01$; ***, $P < 0.001$. Error bars represent the mean ± the SEM.

Table I. Expression of *IL1RL2*, *IL1F6*, and *IL1F5* is increased in psoriatic skin

Gene	PS[a]			NLS[b]			
	No. patients with expression	Mean expression score (range)	SD of score	No. patients with expression	Mean expression score (range)	SD of score	No. patients with PS > NLS
IL1RL2	9/10	0.9 (0–1.0)	0.32	0/10	0	0	9/10
IL1F6	10/10	3.3 (1.5–5.0)	1.38	1/10	0.1 (0–1.0)	0.32	10/10
IL1F5	10/10	2.8 (2.0–3.0)	0.48	10/10	1.8 (1.0–3.0)	0.75	7/10

ISH was performed on skin from 10 psoriasis patients. Both psoriatic and nonlesional skin from the same patients was analyzed. Antisense and sense probes were used, and only the antisense probes gave rise to a positive signal. Staining intensity was scored from 0 (no staining) to 5.0 (very strong staining).
[a]PS, psoriatic skin.
[b]NLS, nonlesional skin.

K14/*IL1F6* pups have skin defects with changes in both keratinocyte proliferation and differentiation. Epidermal hyperplasia is observed as demonstrated by up-regulation of K6 (Fig. 1 C) and phosphorylation of histone H3 (unpublished data) (35). K14/*IL1F6* pups with decreased *IL1F5* gene dosage have more severe epidermal hyperplasia than K14/*IL1F6* pups with a full complement of *IL1F5* (Fig. 5 B). Differentiation defects include expression of K14 in the suprabasal layer in K14/*IL1F6* pups (Fig. 2 E) and parakeratosis observed in K14/*IL1F6*, *IL1F5*$^{-/-}$ pups (Fig. 4 D). Additionally, we have observed an increased number of CD205^{+} Langerhans or dermal dendritic cells, CD3^{+} T lymphocytes, macrophages, and neutrophils in the K14/*IL1F6* pup skin. The inflammation marker ICAM-1 is increased in expression in both basal keratinocytes and in dermal cells. We have demonstrated that inhibition of TNF-α, reduction of neutrophil numbers, or the absence of mature lymphocytes cannot completely block the skin phenotype.

Alterations in the skin caused by K14/*IL1F6* expression are distinct from those generated in K14/*IL1A* and K14/*IL18* transgenic mice. Both K14/*IL1F6* and K14/*IL1A* mice have an increase in the number of dermal macrophages, whereas only the K14/*IL1F6* mice have increases in epidermal thickness and in the number of neutrophils and CD205^{+} cells (11). K14/*IL18* mice have features resembling atopic dermatitis (12), whereas the K14/*IL1F6*, *IL1F5*$^{+/-}$ mice have some similarities with psoriasis, but lack several of its histological hallmarks. In addition, the K14/*IL1A* and K14/*IL18* skin phenotypes first occur in adult mice, whereas the K14/*IL1F6* skin abnormalities occur within 1 wk after birth.

An intriguing feature of the K14/*IL1F6* phenotype is that it arises shortly after birth, is resolved by 3 wk of age, and then spontaneously recurs in 6-mo-old mice. Several factors may contribute to the resolution process. First, it appears that *IL1F6* transgene expression is silenced by P10 (Fig. 2 E). The K14 promoter construct used does have expression differences with the endogenous *KRT14* gene (unpublished data) (36). However, this K14 promoter cassette has been used to generate skin phenotypes that do not resolve (unpublished data) (36, 37). This result suggests that the observed resolution of the K14/*IL1F6* skin phenotype is caused by the RP2/IL-1F axis, and not by the K14 expression cassette. Second, K14/*IL1F6* expression results in increased expression in the skin of the two other agonistic ligands that activate RP2, IL-1F8 and -1F9 (Fig. 2 A). It is possible that the activity of IL-1F8 and -1F9 contribute to the skin phenotype, and that their decreased expression from P1 to 21 could be part of the resolution process. Third, *IL1RL2* expression in the skin is slightly decreased after P3 (Fig. 2 B), and could play a role in resolution. Fourth, there is decreased expression of inflammatory cytokines and chemokines over the time course (Fig. 2 C). Fifth, dramatic developmental changes in the skin occur in the same timeframe that phenotypic resolution is initiated. At this time, epidermal thickness decreases and hair growth is initiated. Interestingly, K14/*IL1F6* mice with reduced *IL1F5* gene dosage have recurrence of skin lesions at 4–6 wk of age, which is months earlier than in K14/*IL1F6*, *IL1F5*$^{+/+}$ mice. Recently, we found that topical administration of 12-*O*-tetradecanoylphorbol-13-acetate to back skin of 8-wk-old K14/*IL1F6* mice results in reactivation of the skin phenotype within 3 d (unpublished data). Therefore, decreased IL-1F5 antagonist gene dosage or topical 12-*O*-tetradecanoylphorbol-13-acetate administration can override the normal resolution process.

K14/*IL1F6*, *IL1F5*$^{+/-}$ and K14/*IL1F6*, *IL1F5*$^{-/-}$ skin have several histological hallmarks of psoriasis, as follows: acanthosis, hyperkeratosis, parakeratosis, intracorneal and intraepithelial pustules, presence of a mixed dermal infiltrate, and dilation of superficial dermal blood vessels. Additionally, *IL1RL2*, *IL1F5*, and *IL1F6* are up-regulated in psoriatic skin compared with nonlesional skin from the same patients. However, several features in the K14/IL-1F6 mice or in K14/IL-1F6, IL-1F5$^{-/-}$ mice are different from those in psoriasis. Histological features present in psoriasis that are lacking in these mice are the presence of rete ridges, the absence of the granular layer, and the predominance of lymphocytes in the infiltrate. In addition, the skin abnormalities in the transgenic mice are independent of mature lymphocytes, which are a critical immune cell type in psoriasis. Also, TNF-α blockade has a modest effect on the K14/*IL1F6* skin phenotype, but is an effective treatment for psoriasis (29).

We hypothesize that the balance between IL-1F agonism and IL-1F5 antagonism is critical in skin inflammation (Fig. 7). Although we describe this model with IL-1F6, it is possible

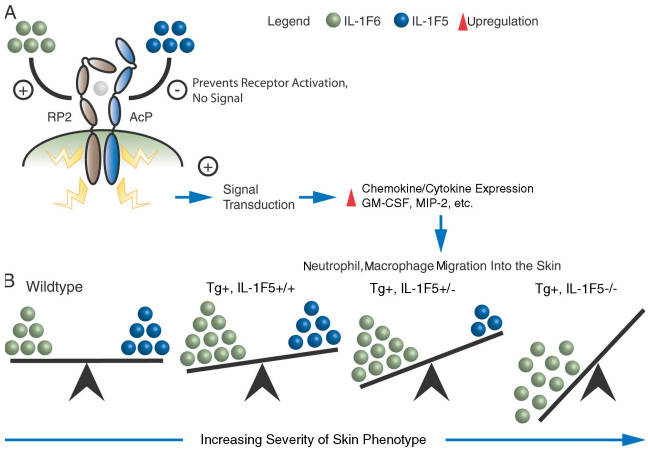

Figure 7. Model for the role of IL-1F6 and -1F5 in the K14/*IL1F6* skin phenotype. (A) Proposed mechanism of action (MOA) for IL-1F6 and -1F5 in the regulation of a competent signaling complex containing RP2 and AcP, and downstream events. IL-1F6 activates a receptor complex, resulting in signal transduction, induction of cytokine and chemokine expression, and mobilization of neutrophils and macrophage into the dermis. This process is antagonized by IL-1F5. (B) Model for the critical balance between IL-1F6 and -1F5 expression in pup skin inflammation. In wild-type pups, a balance between IL-1F6 agonist activity and IL-1F5 antagonist activity results in normal skin. Increasing IL-1F6 expression by transgenic expression in an *IL1F5*$^{+/+}$ background tips the balance toward skin inflammation. Reducing *IL1F5* gene dosage (*IL1F5*$^{+/-}$) in the K14/*IL1F6* mice exacerbates skin inflammation. Complete deletion of *IL1F5* further shifts the balance in K14/*IL1F6* mice, resulting in an even more severe inflammation.

that other IL-1 family ligands are also involved. In the model, IL-1F5 antagonism prevails and inflammation is minimal in the skin of wild-type mice. Shifting the balance to favor IL-1F6 agonism is proposed to result in activation of signaling through RP2/AcP, induction of cytokine and chemokine expression in the skin, and recruitment of neutrophils and macrophages (Fig. 7 A). This can be accomplished by transgenic expression of *IL1F6* and can be further skewed by combining *IL1F6* transgenic expression with decreased expression of *IL1F5* (*IL1F5*$^{+/-}$ or *IL1F5*$^{-/-}$), resulting in a more severe skin pathology (Fig. 7 B). Future studies will be required to understand the role of this axis in human skin disease.

MATERIALS AND METHODS

Plasmid construction. The pHR2 plasmid containing the human K14 (K14) promoter was a kind gift of S. Werner (Institute of Cell Biology, Zurich, Switzerland) (37). The unique Sma1 cloning site for cDNA insertion was converted to an Fse1/Pme1/Asc1 polylinker to create pHB137-9. Mouse *IL1F6* (GenBank accession no. NM_019450) was used as a template for the polymerase chain reaction (PCR) to generate the open reading frame (166–644 in NM_019450) flanked by a 5′ Fse1 site and a consensus translation initiation sequence, and a 3′ Asc1 site directly after the stop codon. This fragment was inserted in pHB137-9 digested with Fse1/Asc1 to yield pHB225-1. Nucleotide sequencing confirmed that the PCR fragment was identical to the template sequence. The K14/mouse *IL1F6*/hGH poly A expression cassette was excised from pHB225-1 with Kpn1, to eliminate bacterial sequences from the microinjection fragment.

Generation of transgenic mice and genetic crosses. The K14/*IL1F6* Kpn1 fragment was microinjected at a concentration of 2 ng/ml in 10 mM Tris and 0.1 mM EDTA, pH 8.0 into the pronuclei of mouse embryos obtained from B6D2F1 female mice bred to B6D2F1 male mice (Taconic), and implanted into pseudopregnant Swiss-Webster (Taconic) recipients. Mice were genotyped by PCR with primers in the human growth hormone (hGH) polyA region to screen for founders. Transgenic expressers were determined using quantitative RT-PCR analysis of tail skin biopsies from 7-wk-old founders. Total tail skin RNA was isolated using the RNAeasy Midi kit (Qiagen). RT-PCR was performed using a Taqman Reverse Transcription Reagents kit (Applied Biosystems). Expression levels were determined by the expression of an *GH1* probe (Amgen) relative to *GAPDH* (Applied Biosystems). The highest expressers were developed into lines by backcrossing to C57BL/6 mice (Taconic). Genotyping for *IL1RL2*, *IL1RAP*, *IL1R1*, *IL1F5*, *TNFRSF1A*, and *RAG2* was by standard PCR procedures.

Mouse sources. *IL1R*-deficient mice on a C57BL/6 background have been previously described (14, 15). C57BL/6 and *RAG2*–deficient mice (B6.129S6-*RAG2*^{tm1Fwa}N12) were obtained from Taconic. *IL1RAP*-deficient mice (B6; 129S1-*Il1rap*^{tm1Rom1}/J) were obtained from Jackson Immuno-Research Laboratories. Mice lacking *IL1RL2* and *IL1F5* were generated by homologous recombination in 129-derived ES cells (Lexicon Genetics). In brief, exons 1–3 of the *IL1F5* gene and exons 2–4 of the *IL1RL2* gene were replaced with a lacZneo cassette. Targeted ES clones were identified by Southern blot analyses and injected into C57BL/6 blastocysts. The resulting chimeras were crossed to C57BL/6 to generate B6;129 F1 heterozygotes, which were intercrossed to generate B6;129 F2 homozygotes. The mutants used throughout these studies are on a random hybrid B6;129 genetic background. All protocols used in these studies were in compliance with federal guidelines and the Amgen Institutional Animal Care and Use Committee.

Quantitative RT-PCR expression analysis. Quantitative RT-PCR was performed using a Taqman Reverse Transcription Reagents kit (Applied Biosystems). Expression levels for the following genes were determined by their expression using the following primers and probes, which were designed in-house (Amgen) relative to mouse *ACTB* (Applied Biosystems): *IL1F5*, *IL1F6*, *IL1F8*, *IL1F9*, *IL1RL2*, *IL23A*, *CSF2*, and *IL1A*. Predesigned Taqman Gene Expression Assays (Applied Biosystems) were used for the following genes: *IL1RAP*, *TNF*, *CCL2*, *KRT14*, *CXCL2*, *TGA2*, *HBEGF*, and *AREG*.

Histopathological analysis. Standard histopathologic examination was performed on skin samples fixed in 10% neutral buffered formalin, processed routinely, and stained with hematoxylin and eosin (HE). IHC was performed on selected skin sections using the following antibodies: 2.5 μg/ml K6 (Covance), 50 ng/ml K14 (Covance), 2 μg/ml CD54 (ICAM-1; Millipore), 10 μg/ml CD205 (DEC205; Serotec), 5 μg/ml CD3 (DakoCytomation), 20 μg/ml F4/80 (BM8; Serotec), and 15 μg/ml IL-1F6 (Amgen). IHC for CD54 and CD205 were performed on skin samples fixed with Zinc-Tris buffer (0.1 M Tris, pH 7.4) rather than formalin because of sensitivity of the antigens to protein cross-linking. All other antibodies were used on formalin-fixed, paraffin-embedded samples. IHC for keratin 6 and F4/80 required antigen retrieval for 5 min with proteinase K.

Epidermal thickness was measured on formalin-fixed, paraffin-embedded samples of back skin stained with HE. For each animal, a digital photographic image was taken using the 20× microscope objective in the area of maximal epidermal thickening, and the epidermal thickness from the bottom of the keratin layer to the epidermal basement membrane was measured in micrometers at three locations on each image using the caliper function of MetaVue morphometry software (Universal Imaging Corporation). The three measurements were averaged to determine the maximal epidermal thickness for each animal. The group mean and SD were calculated using the mean epidermal thickness for each individual as a single value. Skin samples were blinded and mixed randomly before image field selection and while taking epidermal measurements. Inflammation severity ranking was done on

blinded, randomly ordered samples by a subjective evaluation of the severity of inflammatory infiltrate, disregarding epidermal thickness. Samples were ordered from least to most severely inflamed and ranked accordingly so that the sample with the least severe inflammation was given a value of 1, the next most severe given a value of 2, etc, until all samples in an experiment were numbered in order.

Antibodies used in the treatment of K14/*IL1F6* pups. M616, which is a rat IgG2a anti–mouse RP2 blocking antibody, was generated at Amgen. 3F8, which is a rat IgG2a isotype-matched control antibody raised against an irrelevant protein, was also generated at Amgen. Purified rat anti–mouse Ly-6G and Ly-6C (Gr-1, IgG_{2b}, κ isotype) was purchased from BD PharMingen. Purified rat IgG_{2b}, κ isotype-matched control antibody was purchased from BD PharMingen. TN3-19.12, which is a hamster antibody against mouse TNF-α, was purchased from eBioscience. The control antibody for TN3-19.12 was hamster IgG (Pierce Chemical Co.).

Half of the litter was tail snipped so that we could distinguish pups treated with test antibody from those treated with control antibody. Newborn pups were injected intraperitoneally with either 50 μg M616 or with 50 μg of an isotype-matched control antibody (3F8) starting 1 d after birth, every other day for 1 wk. Pups were scored at P7 for a visible skin phenotype and killed, and skin was collected for histopathological analysis. Similar experiments were performed with anti–mouse Ly-6G/Ly-6C (anti-Gr1) versus control antibody, and for anti–TNF-α (TN-3-19.12) versus hamster IgG in newborn K14/*IL1F6* pups.

Quantitation of cytokine and chemokine levels in skin protein extracts. Back skin from individual pups was isolated and immediately frozen in liquid nitrogen. Tissue was converted into powder using a Bessman Tissue Pulverizer (Fisher Scientific). Extracts were homogenized in ice-cold digestion buffer (50 mM Tris, pH 7.4 containing 0.1 M NaCl and 0.1% Triton X-100). The homogenate was centrifuged at 15,000 rpm for 20 min, aliquoted, and stored at −20°C until further analysis. Skin protein extracts were normalized by BCA total protein quantitation kit (Pierce Chemical Co.). Multiple analyte panel (MAP) analysis on skin protein extracts was performed by Rules Based Medicine using Luminex technology. MAP results for specific analytes were validated by ELISA analysis. Mouse MIP-2, GM-CSF, MCP-1, IL-6, and KC were quantified using duosets (R&D Systems). Plates were read using the Vmax Microplate Reader (Molecular Devices).

ISH. A standard ISH protocol was performed using antisense ^{33}P-labeled RNA probes synthesized by in vitro transcription of the template with either T3 or T7 RNA polymerase after linearization of the vector with an appropriate restriction enzyme. The human *IL1F5* probe was 581 nt long, from 131–712, in GenBank accession no. NM_012275. The human *IL1F6* probe was 477 nt long, from 1–477, in GenBank accession no. AF201831. The human *IL1RL2* probe was 1,005 nt long, from 133–1,139, in GenBank accession no. AF284434. Probes were hybridized on tissue sections overnight at 60°C, followed by RNase digestion to remove unhybridized probe and a series of washes, with the highest stringency being 0.1× SSC at 55°C for 30 min. The slides were coated with Kodak NTB2 emulsion and exposed for 3 wk in the dark at 0–4°C, developed, and then counterstained with HE.

Statistical analysis. All statistical calculations were performed using SAS software version 9.1 (SAS Institute, Inc.). In Fig. 1 D, P values were calculated from two-sample *t* tests with unequal variances and further adjusted by Bonferroni procedure for multiple comparisons. In Fig. 1 E, log transformation was applied to the epidermal thickness to improve normality. The nonparametric approach was applied when log transformation failed to improve the normality. P values were calculated from mixed effect models, including genotype and ID (animal) as random effect for each time point. P values were adjusted by Bonferroni procedure for multiple comparisons. In Fig. 2 (A–C), log transformation was applied to the 2E-DCT measurement to improve normality. Differences in gene expression between genotype groups were conducted using analysis of variance by contrasting at each time point. The resultant P values were adjusted using the stepdown Sidak procedure for multiple comparisons by each gene. In Fig. 4 A, P value was calculated by analysis of variance and contrasting between indicated groups. In Fig. 4 (B and C), the effect of genotype on dermal inflammation ranking was tested by a two-sample *t* test. In Fig. 6 D, log transformation was applied to the 2E-DCT to improve normality. Paired *t* tests were used for comparison between PS and NLS on log-transformed IL1RL2 and IL1F5 data. A Wilcoxon signed rank test was used for F6 because of the nonnormal distribution of the data.

We are grateful to Sabine Werner for providing the plasmid containing the human K14 promoter. We thank the following colleagues for their contributions: Dan Branstetter, Bernie Buetow, Keith Charrier, Guang Chen, Mike Comeau, Taska Dobson, Barbara Felder, Chris Gabel, Moira Glaccum, Kari Hale, Deanna Hill, Tenzin Jigme, Keith Kerkoff, Bill Lawrence, Melissa Lee, Michelle Pace, Lori Petersen, Blair Renshaw, Dirk Smith, Cheng Su, and Jeffrey Williams. We acknowledge generation of the *IL1RL2*- and *IL1F5*-deficient mice by Lexicon Genetics. We thank the Inflammation Therapeutic Area at Amgen for critical analysis of this work. We dedicate this manuscript to the memory of our colleague Brad Sevetson.

All authors, except M.K. Kuechle, were employees of Amgen and/or Immunex Corporation (acquired by Amgen) at the time of this research. Authors that are current Amgen employees are shareholders in the company. This could be considered to pose a financial conflict of interest regarding the submission of this manuscript. The authors have no other competing financial interests.

Submitted: 19 January 2007
Accepted: 7 September 2007

REFERENCES

1. Sims, J.E., M.J. Nicklin, J.F. Bazan, J.L. Barton, S.J. Busfield, J.E. Ford, R.A. Kastelein, S. Kumar, H. Lin, J.J. Mulero, et al. 2001. A new nomenclature for IL-1-family genes. *Trends Immunol.* 22:536–537.
2. Sims, J.E. 2002. IL-1 and IL-18 receptors, and their extended family. *Curr. Opin. Immunol.* 14:117–122.
3. Greenfeder, S.A., P. Nunes, L. Kwee, M. Labow, R.A. Chizzonite, and G. Ju. 1995. Molecular cloning and characterization of a second subunit of the interleukin 1 receptor complex. *J. Biol. Chem.* 270:13757–13765.
4. Eisenberg, S.P., M.T. Brewer, E. Verderber, P. Heimdal, B.J. Brandhuber, and R.C. Thompson. 1991. Interleukin 1 receptor antagonist is a member of the interleukin 1 gene family: evolution of a cytokine control mechanism. *Proc. Natl. Acad. Sci. USA.* 88:5232–5236.
5. Re, F., M. Sironi, M. Muzio, C. Matteucci, M. Introna, S. Orlando, G. Penton-Rol, S.K. Dower, J.E. Sims, F. Colotta, et al. 1996. Inhibition of interleukin-1 responsiveness by type II receptor gene transfer: a surface "receptor" with anti-interleukin-1 function. *J. Exp. Med.* 183:1841–1850.
6. Smith, D.E., R. Hanna, D. Friend, H. Moore, H. Chen, A.M. Farese, T.J. Mac Vittie, G.D. Virca, and J.E. Sims. 2003. The soluble form of IL-1 receptor accessory protein enhances the ability of soluble type II IL-1 receptor to inhibit IL-1 action. *Immunity.* 18:87–96.
7. Dinarello, C.A. 1999. IL-18: A Th1-inducing, proinflammatory cytokine and new member of the IL-1 family. *J. Allergy Clin. Immunol.* 103:11–24.
8. Akira, S. 2000. The role of IL-18 in innate immunity. *Curr. Opin. Immunol.* 12:59–63.
9. Born, T.L., E. Thomassen, T.A. Bird, and J.E. Sims. 1998. Cloning of a novel receptor subunit, AcPL, required for interleukin-18 signaling. *J. Biol. Chem.* 273:29445–29450.
10. Novick, D., S.H. Kim, G. Fantuzzi, L.L. Reznikov, C.A. Dinarello, and M. Rubinstein. 1999. Interleukin-18 binding protein: a novel modulator of the Th1 cytokine response. *Immunity.* 10:127–136.
11. Groves, R.W., H. Mizutani, J.D. Kieffer, and T.S. Kupper. 1995. Inflammatory skin disease in transgenic mice that express high levels of interleukin 1 alpha in basal epidermis. *Proc. Natl. Acad. Sci. USA.* 92:11874–11878.
12. Kawase, Y., T. Hoshino, K. Yokota, A. Kuzuhara, Y. Kirii, E. Nishiwaki, Y. Maeda, J. Takeda, M. Okamoto, S. Kato, et al. 2003. Exacerbated and prolonged allergic and non-allergic inflammatory

cutaneous reaction in mice with targeted interleukin-18 expression in the skin. *J. Invest. Dermatol.* 121:502–509.
13. Shepherd, J., M.C. Little, and M.J.H. Nicklin. 2004. Psoriasis-like cutaneous inflammation in mice lacking interleukin-1 receptor antagonist. *J. Invest. Dermatol.* 122:665–669.
14. Labow, M., D. Shuster, M. Zetterstrom, P. Nunes, R. Terry, E.B. Cullinan, T. Bartfai, C. Solorzano, L.L. Moldawer, R. Chizzonite, et al. 1997. Absence of IL-1 signaling and reduced inflammatory response in IL-1 type I receptor-deficient mice. *J. Immunol.* 159:2452–2461.
15. Glaccum, M.B., K.L. Stocking, K. Charrier, J.L. Smith, C.R. Willis, C. Maliszewski, D.J. Livingston, J.J. Peschon, and P.J. Morrissey. 1997. Phenotypic and functional characterization of mice that lack the type I receptor for IL-1. *J. Immunol.* 159:3364–3371.
16. Cullinan, E.B., L. Kwee, P. Nunes, D.J. Shuster, G. Ju, K.W. McIntyre, R.A. Chizzonite, and M.A. Labow. 1998. IL-1 receptor accessory protein is an essential component of the IL-1 receptor. *J. Immunol.* 161:5614–5620.
17. Hoshino, K., H. Tsutsui, T. Kawai, K. Takeda, K. Nakanishi, Y. Takeda, and S. Akira. 1999. Cutting edge: generation of IL-18 receptor-deficient mice: evidence for IL-1 receptor-related protein as an essential IL-18 binding receptor. *J. Immunol.* 162:5041–5044.
18. Cheung, H., N.J. Chen, Z. Cao, N. Ono, P.S. Ohashi, and W.C. Yeh. 2005. Accessory protein-like is essential for IL-18-mediated signaling. *J. Immunol.* 174:5351–5357.
19. Mulero, J.J., A.M. Pace, S.T. Nelken, D.B. Loeb, T.R. Correa, R. Drmanac, and J.E. Ford. 1999. IL1HY1: A novel interleukin-1 receptor antagonist gene. *Biochem. Biophys. Res. Commun.* 263:702–706.
20. Lin, H., A.S. Ho, D. Haley-Vicente, J. Zhang, J. Bernal-Fussell, A.M. Pace, D. Hansen, K. Schweighofer, N.K. Mize, and J.E. Ford. 2001. Cloning and characterization of IL-1HY2, a novel interleukin-1 family member. *J. Biol. Chem.* 276:20597–20602.
21. Smith, D.E., B.R. Renshaw, R.R. Ketchem, M. Kubin, K.E. Garka, and J.E. Sims. 2000. Four new members expand the interleukin-1 superfamily. *J. Biol. Chem.* 275:1169–1175.
22. Kumar, S., P.C. McDonnell, R. Lehr, L. Tierney, M.N. Tzimas, D.E. Griswold, E.A. Capper, R. Tal-Singer, G.I. Wells, M.L. Doyle, et al. 2000. Identification and initial characterization of four novel members of the interleukin-1 family. *J. Biol. Chem.* 275:10308–10314.
23. Dunn, E., J.E. Sims, M.J.H. Nicklin, and L.A.J. O'Neill. 2001. Annotating genes with potential roles in the immune system: six new members of the IL-1 family. *Trends Immunol.* 22:533–536.
24. Taylor, S.L., B.R. Renshaw, K.E. Garka, D.E. Smith, and J.E. Sims. 2002. Genomic organization of the interleukin-1 locus. *Genomics.* 79:726–733.
25. Nicklin, M.J.H., J.L. Barton, M. Nguyen, M.G. FitzGerald, G.W. Duff, and K. Kornman. 2002. A sequence-based map of the nine genes of the human interleukin-1 cluster. *Genomics.* 79:718–725.
26. Lovenberg, T.W., P.D. Crowe, C. Liu, D.T. Chalmers, X.J. Liu, C. Liaw, W. Clevenger, T. Oltersdorf, E.B. De Souza, and R.A. Maki. 1996. Cloning of a cDNA encoding a novel interleukin-1 receptor related protein (IL 1R-rp2). *J. Neuroimmunol.* 70:113–122.
27. Debets, R., J.C. Timans, B. Homey, S. Zurawski, T.R. Sana, S. Lo, J. Wagner, G. Edwards, T. Clifford, S. Menon, et al. 2001. Two novel IL-1 family members, IL-1 delta and IL-1 epsilon, function as an antagonist and agonist of NF-kappa B activation through the orphan IL-1 receptor-related protein 2. *J. Immunol.* 167:1440–1446.
28. Towne, J.E., K.E. Garka, B.R. Renshaw, G.D. Virca, and J.E. Sims. 2004. Interleukin (IL)-1F6, IL-1F8, and IL-1F9 signal through IL-1Rrp2 and IL-1RacP to activate the pathway leading to NF-kappaB and MAPKs. *J. Biol. Chem.* 279:13677–13688.
29. Victor, F.C., A.B. Gottlieb, and A. Menter. 2003. Changing paradigms in dermatology: tumor necrosis factor alpha (TNF-alpha) blockade in psoriasis and psoriatic arthritis. *Clin. Dermatol.* 21:392–397.
30. Sheehan, K.C., N.H. Ruddle, and R.D. Schreiber. 1989. Generation and characterization of hamster monoclonal antibodies that neutralize murine tumor necrosis factors. *J. Immunol.* 142:3884–3893.
31. Schon, M., D. Denzer, R.C. Kubitza, T. Ruzicka, and M.P. Schon. 2000. Critical role of neutrophils for the generation of psoriasiform skin lesions in flaky skin mice. *J. Invest. Dermatol.* 114:976–983.
32. Shinkai, Y., G. Rathbun, K.P. Lam, E.M. Oltz, V. Stewart, M. Mendelsohn, J. Charron, M. Datta, F. Young, A.M. Stall, et al. 1992. RAG-2-deficient mice lack mature lymphocytes owing to inability to initiate V(D)J rearrangement. *Cell.* 68:855–867.
33. Hardman, M.J., P. Sisi, D.N. Banbury, and C. Byrne. 1998. Patterned acquisition of skin barrier function during development. *Development.* 125:1541–1552.
34. Schmitz, J., A. Owyang, E. Oldham, Y. Song, E. Murphy, T.K. McClanahan, G. Zurawski, M. Moshrefi, J. Qin, X. Li, et al. 2005. IL-33, an interleukin-1-like cytokine that signals via the IL-1 receptor-related protein ST2 and induces T helper type 2-associated cytokines. *Immunity.* 23:479–490.
35. Ribalta, T., I.E. McCutcheon, K.D. Aldape, J.M. Bruner, and G.N. Fuller. 2004. The mitosis-specific antibody anti-phosphohistone-H3 (PHH3) facilitates rapid reliable grading of meningiomas according to WHO 2000 criteria. *Am. J. Surg. Pathol.* 28:1532–1536.
36. Sil, A.K., S. Maeda, Y. Sano, D.R. Roop, and M. Karin. 2004. IκB kinase-α acts in the epidermis to control skeletal and craniofacial morphogenesis. *Nature.* 428:660–664.
37. Munz, B., H. Smola, F. Engelhardt, K. Bleuel, M. Brauchle, I. Lein, L.W. Evans, D. Huylebroeck, R. Balling, and S. Werner. 1999. Overexpression of activin A in the skin of transgenic mice reveals new activities of activin in epidermal morphogenesis, dermal fibrosis and wound repair. *EMBO J.* 18:5205–5215.